

Superstructure and physical properties of skutterudite-related phase $\text{CoGe}_{1.5}\text{Se}_{1.5}$

Y Liang, B Fang, X M Zhu and M M Liang

Institute of Nuclear Technology and Application, School of Science, East China University of Science and Technology, Meilong Road 130, Shanghai 200237, China

E-mail: yliang@ecust.edu.cn

Abstract. $\text{CoGe}_{1.5}\text{Se}_{1.5}$ skutterudite-related phase with a homogeneity range has been synthesized by solid-state reaction. The phase purity, homogeneity range, crystal structure, thermal stability and electrical resistivity were studied. XRD data indicates that $\text{CoGe}_{1.5}\text{Se}_{1.5}$ crystallized in a modification of the skutterudite CoAs_3 type structure with space group $R\bar{3}$ ($a = b = 11.751(1)$ Å, $c = 14.36(1)$ Å). HRTEM-SAED shows more information about the superstructure to confirm the rhombohedral symmetry with space group $R\bar{3}$. The lattice parameter of this skutterudite-related phase was found to be dependent on the concentration of Ge and Se. $\text{CoGe}_{1.5}\text{Se}_{1.5}$ decomposed between 1073 K and 1173 K under argon atmosphere investigated by in-situ XRD, suggesting a good thermal stability. $\text{CoGe}_{1.49}\text{Se}_{1.42}$, $\text{CoGe}_{1.43}\text{Se}_{1.34}$ and $\text{CoGe}_{1.50}\text{Se}_{1.15}$ dense bulk samples were obtained by hot-press technique. The chemical composition detected by FESEM/EDS suggests the homogeneity range and the existence of voids at framework positions. The electrical resistivity of the compounds decreases with increasing temperature, acting as a semiconductor. The chemical composition has a big influence on the value of electrical resistivity and energy gap.

Keywords: related skutterudite, $\text{CoGe}_{1.5}\text{Se}_{1.5}$, superstructure, electrical resistivity

1. Introduction

Since the natural mineral CoAs_3 was first found in 1845 by Wilhelm von Haidinger at Skutterud, Norway, this structure class of MPn_3 ($M = \text{Co, Rh, Ir}$; $Pn = \text{P, As, Sb}$) was named as skutterudite [1]. The skutterudite compounds crystallize in a body-centered cubic with space group $Im\bar{3}$. The pnictogen atoms framework located at the $24g$ sites offers several types of voids which can be filled by guest atoms. As shown in figure 1, the octahedral voids are filled by transitional metal atoms at $8c$ sites, forming tilted corner-sharing octahedrons [MPn_6]. In some cases, the icosahedral voids can be filled by electropositive atoms at $2a$ sites, giving rise to filled skutterudites of general formula, $R_xM_4Pn_{12}$ ($R = \text{alkali metal, alkaline earth metal and rare earth metal}$). In addition to the unfilled binary and filled ternary skutterudites, another group of materials with skutterudite-related structure exists. These compounds, also known as ternary but unfilled skutterudites, are obtained by simultaneous substitution of group 14 and 16 atoms on the pnictogen sites with general formula of $MT_{1.5}Ch_{1.5}$ ($T = \text{Si, Ge and Sn}$; $Ch = \text{S, Se and Te}$). The skutterudite-related phase behaves complex crystal structure because of a distortion of the anion sublattice, as well as various physical properties due to its large variety of compositions.



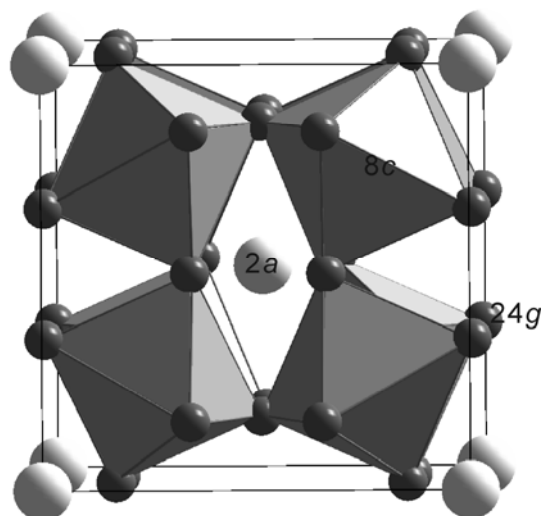


Figure 1. Crystal structure of skutterudite.

For the crystallographic studies, an ordered variant of the skutterudite structure was discussed for $\text{CoGe}_{1.5}\text{S}_{1.5}$ by Wold et al. from additional superstructure reflections in the X-ray powder diffraction pattern [2]. Then they suggested a short-range ordering of group 14 and 16 anions in primitive cubic model for $\text{IrGe}_{1.5}\text{S}_{1.5}$, $\text{IrGe}_{1.5}\text{Se}_{1.5}$, $\text{IrSn}_{1.5}\text{S}_{1.5}$ and $\text{RhGe}_{1.5}\text{S}_{1.5}$ [3]. Lutz et al. proposed the space group $R\bar{3}$ for $\text{CoGe}_{1.5}\text{Ch}_{1.5}$ ($\text{Ch} = \text{S}, \text{Se}$) from single crystal data of a pseudo-merohedral twin [4] and their model explained the superstructure. Later, Vaqueiro et al. found a center of inversion for the proposed crystal structure from the X-ray powder study on $\text{CoGe}_{1.5}\text{Te}_{1.5}$ [5]. Since then, all anion substituted ternary skutterudites, $\text{MT}_{1.5}\text{Ch}_{1.5}$ ($M = \text{Co}, \text{Rh}$ and Ir ; $T = \text{Ge}$ and Sn ; $\text{Ch} = \text{S}, \text{Se}$ and Te), have been refined in the space group $R\bar{3}$ from X-ray or neutron powder diffraction data [6-11]. Recently, Wehrich et al. refined the crystal structure of $\text{IrSn}_{1.5}\text{Se}_{1.5}$ in space group $R\bar{3}$ from single crystal data [12]. For electronic properties, the related skutterudites should be semiconductors, as they are isoelectronic with CoSb_3 . In fact, the electrical resistivity data of $\text{CoGe}_{1.5}\text{S}_{1.5}$, $\text{RhGe}_{1.5}\text{S}_{1.5}$ [7], $\text{CoGe}_{1.5}\text{Se}_{1.5}$ [13], $\text{RhGe}_{1.5}\text{Se}_{1.5}$ [10] and $\text{CoGe}_{1.5}\text{Te}_{1.5}$ [11] showed semiconducting temperature dependences. $\text{CoSn}_{1.5}\text{Se}_{1.5}$ [8], $\text{RhSn}_{1.5}\text{Te}_{1.5}$ and $\text{IrSn}_{1.5}\text{Te}_{1.5}$ [6, 14] behaved as semiconductors at low temperature, while showed metal-like behavior above 300 K. In addition, Nolas et al. reported that $\text{CoGe}_{1.452}\text{Se}_{1.379}$ and $\text{CoGe}_{1.431}\text{Se}_{1.385}$ is n-type and p-type semiconductor, respectively, because of the different concentration of Ge and Se [15]. Liang et al. found that the Ge/Se ratios significantly affected the electrical resistivity of $\text{RhGe}_x\text{Se}_{3-x}$ [10]. However, no detailed information concerning the homogeneity and superstructure of $\text{CoGe}_{1.5}\text{Se}_{1.5}$ is available.

Herein, $\text{CoGe}_{1.5}\text{Se}_{1.5}$ skutterudite-related phase with a homogeneity range has been synthesized by solid-state reaction and hot-press treatment. The phase purity, homogeneity range, superstructure, thermal stability and electrical resistivity were studied.

2. Synthesis and Characterization

The samples of $\text{CoGe}_x\text{Se}_{3-x}$ ($1.0 \leq x \leq 2.0$) were prepared from powdered Co (Chempur, 99.9%), Ge (Chempur, 99.999%) and Se (Chempur, 99.99%). Stoichiometric amounts of starting materials about 2 g were mixed and pressed to pellets. The pellets were sealed in vacuum silica tubes (10^{-3} Pa), annealed at 873 K for 5 d and quenched in water to room temperature. The products were stable in air and water. The so obtained samples after solid-state reaction were ground to fine powder and loaded into graphite dies of inner diameter 10 mm for hot-press treatment. Densification was achieved by heating to 823 K at 30 K/min under a uniaxial pressure of 100 MPa in argon atmosphere. After a reaction time of 30 minutes, the samples were cooled down to room temperature. The pellets obtained were cut with a diamond wire-saw for the electrical resistivity measurements.

For phase analysis and determination of unit cell parameters, data were collected with a D/MAX-2550 diffractometer (Rigaku, Cu $K\alpha$, $10^\circ \leq 2\theta \leq 80^\circ$, $\Delta 2\theta = 0.02^\circ$). Unit cell parameters were calculated from reflection positions determined by profile deconvolution with the program package WinCSD [16] and corrected with internal LaB₆ standard (NIST, $a = 4.15692(1)$ Å). The in-situ X-ray powder diffraction was performed on a DX-2700A diffractometer (Cu $K\alpha$, $10^\circ \leq 2\theta \leq 80^\circ$, $\Delta 2\theta = 0.02^\circ$). The sample was heated stepwise from 293 K to 1273 K (heating rate ≈ 50 K/min, holding time at each temperature before collecting data ≈ 5 min) under argon. Specimens for TEM investigations were prepared by dispersing and crushing small amounts of powder in ethanol, and then deposited on holey carbon support films on copper grids. A JEOL JEM-2100F electron microscope was used. The selected area electron diffraction (SAED) method was performed on thin particles for unit cell characterization. Energy-Dispersive X-ray spectroscopy (EDS) was performed with a Hitachi S-4800 field emission scanning electron microscope. Electrical resistivity was measured on hot-pressed samples in a PPMS in the temperature range 2.5 K – 400 K using a four-point method.

3. Results and Discussion

The X-ray powder diffraction pattern of CoGe_{1.5}Se_{1.5} revealed the pure skutterudite-related phase (figure 2). Comparing with the calculated X-ray diffraction pattern in body-centered cubic model with space group $Im\bar{3}$, in the XRD pattern of CoGe_{1.5}Se_{1.5} in fact superstructure reflections with low intensities were visible. The superstructure reflections at $2\theta = 32.30^\circ$, 35.84° , 44.96° , 47.67° , 50.28° , 59.94° , 64.36° and 72.91° correspond to the (131), (223), (413), (241), (333), ($\bar{1}65$), (351) and (437) planes of the rhombohedral crystal structure with space group $R\bar{3}$, respectively. The lattice parameter of CoGe_{1.5}Se_{1.5} is $a = b = 11.751(1)$ Å, $c = 14.36(1)$ Å.

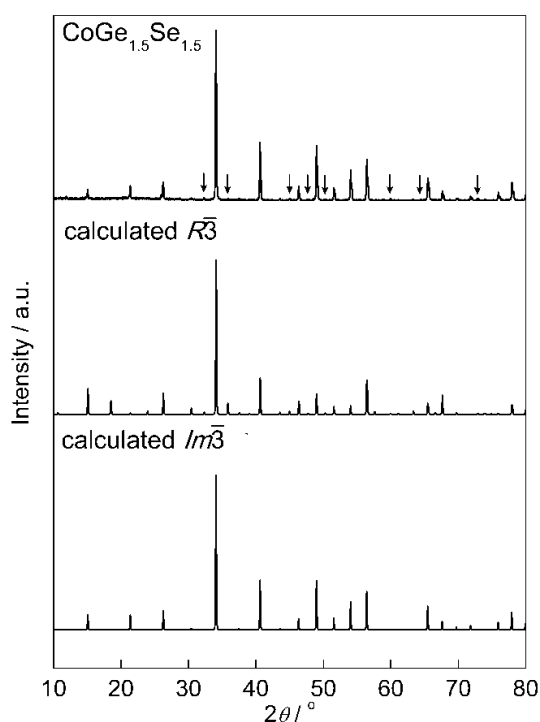


Figure 2. XRD pattern of synthesized CoGe_{1.5}Se_{1.5} powder, calculated patterns for CoGe_{1.5}Se_{1.5} with space group $Im\bar{3}$ and $R\bar{3}$, respectively. Arrows mark weak superstructure reflections.

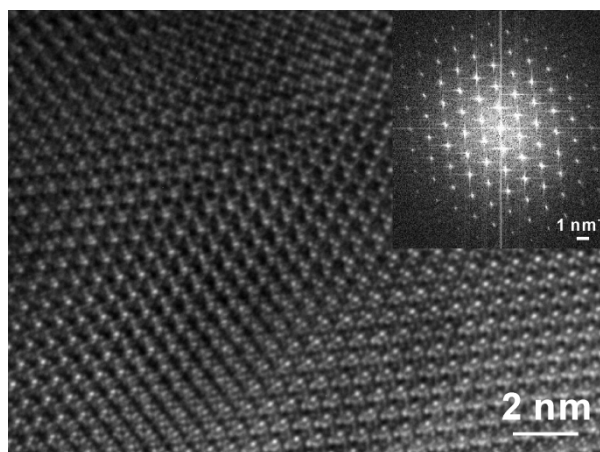


Figure 3. HRTEM and FFT (inset) images of CoGe_{1.5}Se_{1.5} view along [001] direction.

HRTEM investigations of $\text{CoGe}_{1.5}\text{Se}_{1.5}$ reveal particles with large crystalline domains of the skutterudite-related phase (figure 3). To further confirm the superstructure and obtain more information about the symmetry, SAED patterns along different directions were studied (figure 4). At first, the analysis was performed in the original body-centered cubic model with space group $Im\bar{3}$. In this case, Figure 4(a) matches the SAED patterns along $[111]$ direction. The electron diffraction spots with the same spacing distance of $d = 5.876 \text{ \AA}$ correspond to the $(\bar{1}01)$, $(10\bar{1})$, $(\bar{1}10)$, $(1\bar{1}0)$, $(01\bar{1})$ and $(0\bar{1}1)$ planes. While, there are not planes match the typical electron diffraction spots with spacing distances of $d = 8.303 \text{ \AA}$, 5.867 \AA , 4.796 \AA and 4.787 \AA , as shown in figure 4(b). As a consequence, the rhombohedral model with space group $R\bar{3}$ was applied. According to this model, figure 4(a) is the SAED patterns along $[001]$ direction. The electron diffraction spots with the spacing distance of $d = 5.876 \text{ \AA}$ correspond to the (110) , $(\bar{1}\bar{1}0)$, $(2\bar{1}0)$, $(\bar{2}10)$, $(1\bar{2}0)$ and $(\bar{1}20)$ planes. Along $[100]$ direction, the electron diffraction spots with spacing distances of $d = 8.303 \text{ \AA}$, 5.867 \AA , 4.796 \AA and 4.787 \AA correspond to the planes of $(01\bar{1})$, (012) , (021) and (003) , respectively (figure 4(b)). Figure 4(c) presents the SAED patterns along $[1\bar{1}\bar{1}]$ direction. The typical electron diffraction spots with spacing distances of $d = 8.303 \text{ \AA}$, 5.876 \AA and 5.867 \AA represent the (101) , (110) and $(\bar{1}1\bar{2})$ planes, respectively. In the SAED patterns along $[0\bar{2}1]$ direction (figure 4(d)), the marked spots confirm the existence of (012) , (300) and $(\bar{3}12)$ planes with spacing distances of $d = 5.867 \text{ \AA}$, 3.392 \AA and 3.391 \AA , respectively. The results indicate that the SAED patterns along (001) , (100) , $(1\bar{1}\bar{1})$ and $(0\bar{2}1)$ directions consist well with the rhombohedral crystal structure.

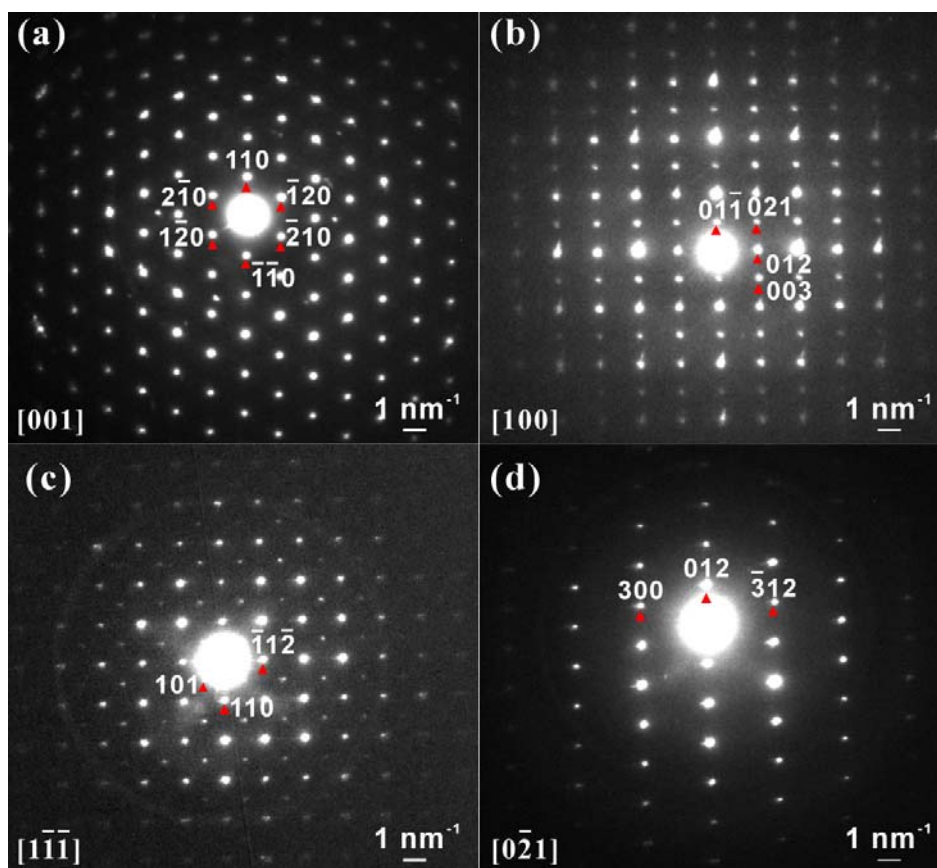


Figure 4. HRTEM-SAED patterns of synthesized $\text{CoGe}_{1.5}\text{Se}_{1.5}$ powder along (a) $[001]$, (b) $[100]$, (c) $[1\bar{1}\bar{1}]$ and (d) $[0\bar{2}1]$ directions.

In order to determine the homogeneity range, samples with different nominal compositions of $\text{CoGe}_x\text{Se}_{3-x}$ ($1.0 \leq x \leq 2.0$) were prepared by solid-state reaction. XRD patterns showed only

reflections of the skutterudite-related phase for $1.3 \leq x \leq 1.8$ samples. Besides skutterudite-related main phase, some elemental Ge in $x \geq 1.9$ samples, or CoSe_2 in $x \leq 1.2$ samples were also investigated in XRD patterns (not shown). Despite of the large range of nominal compositions, unit cell refinement showed only small differences in the lattice parameters (table 1).

Table 1. Nominal composition and lattice parameters of $\text{CoGe}_x\text{Se}_{3-x}$ ($1.3 \leq x \leq 1.8$) skutterudite-related phase.

Nominal composition	Lattice parameters / Å
$\text{CoGe}_{1.3}\text{Se}_{1.7}$	$a = b = 11.750(2), c = 14.40(2)$
$\text{CoGe}_{1.4}\text{Se}_{1.6}$	$a = b = 11.744(2), c = 14.35(3)$
$\text{CoGe}_{1.5}\text{Se}_{1.5}$	$a = b = 11.751(1), c = 14.36(1)$
$\text{CoGe}_{1.6}\text{Se}_{1.4}$	$a = b = 11.741(3), c = 14.43(3)$
$\text{CoGe}_{1.7}\text{Se}_{1.3}$	$a = b = 11.749(2), c = 14.32(3)$
$\text{CoGe}_{1.8}\text{Se}_{1.2}$	$a = b = 11.750(3), c = 14.28(4)$

The in-situ XRD performed on the sample with nominal composition $\text{CoGe}_{1.5}\text{Se}_{1.5}$ exhibited the cell expansion with increasing temperature of the skutterudite-related phase. On heating from 293 K to 1173 K a shift of the reflection positions to lower diffraction angles was observed (figure 5). The lattice parameter of the skutterudite-related phase in this temperature range increased linearly (figure 6). At 1173 K, additional reflections corresponding to some impurities were observed and became clearer at 1273 K, indicating that the decomposed temperature was between 1073 K and 1173 K.

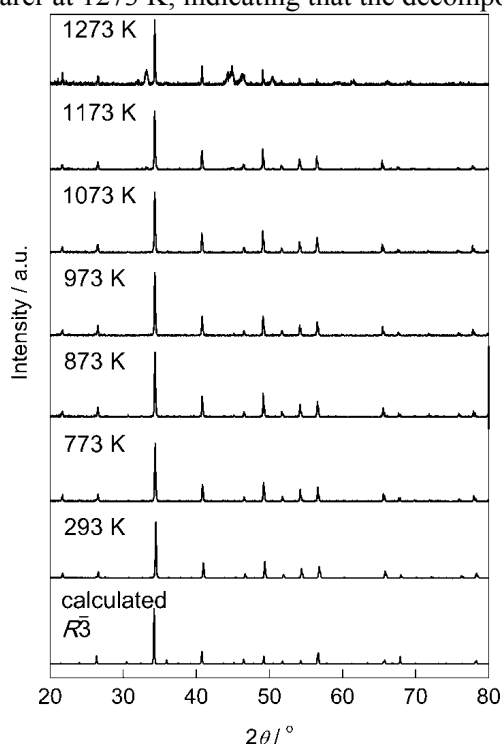


Figure 5. XRD patterns collected in-situ on heating $\text{CoGe}_{1.5}\text{Se}_{1.5}$ powder.

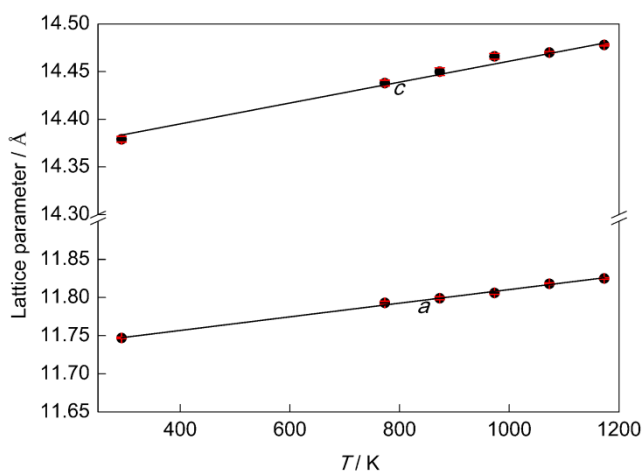


Figure 6. Temperature dependence of the unit cell parameters of $\text{CoGe}_{1.5}\text{Se}_{1.5}$. Error bars lie within the points.

The obtained three samples with nominal compositions of $\text{CoGe}_{1.4}\text{Se}_{1.6}$, $\text{CoGe}_{1.5}\text{Se}_{1.5}$ and $\text{CoGe}_{1.6}\text{Se}_{1.4}$ were further treated by hot-press technique. The preparation resulted in dark-gray bulk with at least 95 % of the theoretical density. XRD patterns reveal the skutterudite-related main phase with some binary GeSe or elemental Ge byproducts (figure 7). The composition of the main phase is $\text{CoGe}_{1.49}\text{Se}_{1.42}$, $\text{CoGe}_{1.43}\text{Se}_{1.34}$ and $\text{CoGe}_{1.50}\text{Se}_{1.15}$, respectively, established by EDS analysis, whereby it

was assumed that the $8c$ positions were completely occupied by cobalt atoms (table 2). The results suggest the homogeneity range of chemical composition, as well as the existence of vacancies at the framework. For all the three samples $\text{CoGe}_{1.49}\text{Se}_{1.42}$, $\text{CoGe}_{1.43}\text{Se}_{1.34}$ and $\text{CoGe}_{1.50}\text{Se}_{1.15}$, the resistivity decreases with increasing temperature from 2.5 K to 400 K confirming the semiconducting behavior of materials (figure 8). The value of electrical resistivity at 300 K is $1.8 \times 10^{-3} \Omega\text{m}$, $6.6 \times 10^{-3} \Omega\text{m}$ and $3.0 \times 10^{-2} \Omega\text{m}$, respectively. The difference increases with decreasing temperature. The much higher electrical resistivity observed for $\text{CoGe}_{1.50}\text{Se}_{1.15}$ perhaps is due to its lower carrier mobility or concentration than that of $\text{CoGe}_{1.49}\text{Se}_{1.42}$ and $\text{CoGe}_{1.43}\text{Se}_{1.34}$. The data at higher temperature (300 K – 400 K) can be fitted by the Arrhenius activation law $\ln(\rho) = \text{constant} + E_g/2k_B T$, where E_g is the energy gap, resulting in $E_g = 0.194$ eV, 0.182 eV and 0.538 eV for $\text{CoGe}_{1.49}\text{Se}_{1.42}$, $\text{CoGe}_{1.43}\text{Se}_{1.34}$ and $\text{CoGe}_{1.50}\text{Se}_{1.15}$, respectively (table 2), comparable with that for $\text{CoGe}_{1.452}\text{Se}_{1.379}$ (0.336 eV) in *ref.* 15. The results indicate that the estimated intrinsic band gap strongly depends on the concentrations.

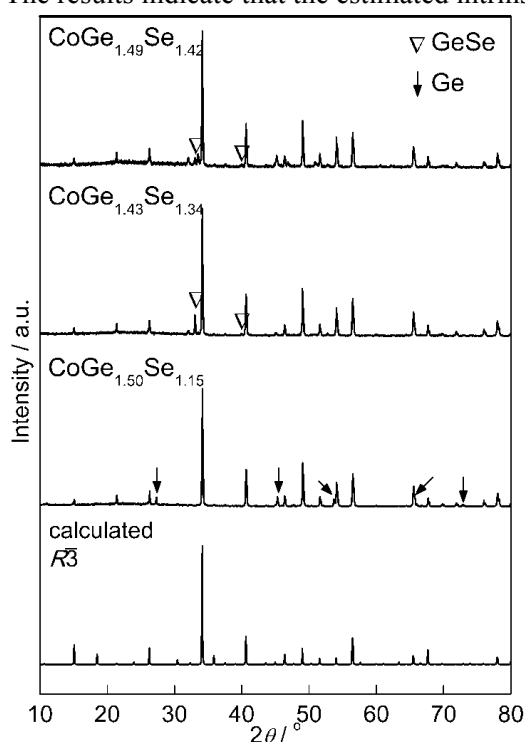


Figure 7. XRD patterns of hot-press treated $\text{CoGe}_{1.49}\text{Se}_{1.42}$, $\text{CoGe}_{1.43}\text{Se}_{1.34}$ and $\text{CoGe}_{1.50}\text{Se}_{1.15}$ samples, calculated pattern with space group $R\bar{3}$.

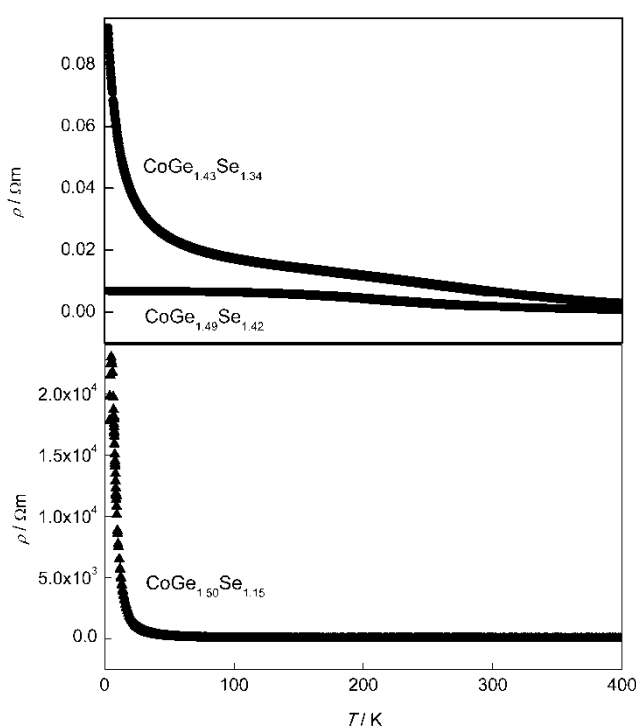


Figure 8. Temperature dependence of the electrical resistivity of $\text{CoGe}_{1.49}\text{Se}_{1.42}$, $\text{CoGe}_{1.43}\text{Se}_{1.34}$ and $\text{CoGe}_{1.50}\text{Se}_{1.15}$.

Table 2. FESEM/EDS results and energy gap (E_g) of hot-press treated samples.

Nominal composition	Composition of main phase from FESEM/EDS	E_g (eV)
$\text{CoGe}_{1.4}\text{Se}_{1.6}$	$\text{Co}_{1.00(5)}\text{Ge}_{1.49(6)}\text{Se}_{1.42(3)}$	0.194
$\text{CoGe}_{1.5}\text{Se}_{1.5}$	$\text{Co}_{1.00(1)}\text{Ge}_{1.43(4)}\text{Se}_{1.34(3)}$	0.182
$\text{CoGe}_{1.6}\text{Se}_{1.4}$	$\text{Co}_{1.00(4)}\text{Ge}_{1.50(6)}\text{Se}_{1.15(9)}$	0.538

4. Conclusions

The skutterudite-related phase $\text{CoGe}_x\text{Se}_{3-x}$ with a homogeneity range has been synthesized by solid-state reaction. XRD shows weak superstructure reflections for all concentrations. More information about superstructure obtained from SAED confirms the rhombohedral crystal structure with space

group $R\bar{3}$. The concentration of Ge and Se detected by EDS suggests the existence of vacancies at the framework positions. The electrical resistivity of $\text{CoGe}_x\text{Se}_{3-x}$ for different concentrations increases with decreasing temperature, indicating a semiconducting behavior of the material. The band gap significantly depends on the concentration.

Acknowledgments

This work was supported by the National Natural Science Foundation of China (Grant number: 51301071), the Innovation Program of Shanghai Municipal Education Commission (Grant number: 14ZZ057).

References

- [1] Haidinger W 1845 *Handbuch der Bestimmenden Mineralogie* (Wien: Braumüller und Seidel)
- [2] Korenstein R, Soled S, Wold A and Collin G 1977 *Inorg. Chem.* **16** 2344
- [3] Lyons A, Gruska R P, Case C, Subbarao S N and Wold A 1978 *Mater. Res. Bull.* **13** 125
- [4] Partik M, Kringe C and Lutz H D 1996 *Z. Kristallogr.* **211** 304
- [5] Vaqueiro P, Sobany G G, Powell A V and Knight K S 2006 *J. Solid State Chem.* **179** 2047
- [6] Bos J W G and Cava R J 2007 *Solid State Commun* **141** 38
- [7] Vaqueiro P, Sobany G G and Stindl M 2008 *J. Solid State Chem.* **181** 768
- [8] Laufek F, Navrátil J, Plášil J, Plecháček T and Drašar Č 2009 *J. Alloys Compd.* **479** 102
- [9] Vaqueiro P, Sobany G G and Powell A V 2010 *Dalton Trans.* **39** 1020
- [10] Liang Y, Schnelle W, Oeschler N, Budnyk S and Grin Yu 2011 *Z. Kristallogr.* **226** 62
- [11] Kaltzoglou A, Powell AV, Knight K S and Vaqueiro P 2013 *J. Solid State Chem.* **198** 525
- [12] Yan W, Pielhofer F, Tragl S A and Wehrich R 2015 *Z. Anorg. Allg. Chem.* **641** 543
- [13] Wei K, Dong Y, Puneet P, Tritt T M and Nolas G S 2014 *J. Alloys Compd.* **614** 330
- [14] Zevalkink A, Star K, Aydemir U, Snyder G J, Fleurial J P, Bux S and Vo T von Allmen P 2015 *J. Appl. Phys.* **118** 035107
- [15] Nolas G S, Yang J and Ertenberg R W 2003 *Phys. Rev. B* **68** 193206
- [16] Akselrud L and Grin Yu 2014 *J. Appl. Cryst.* **47** 803